J Incl Phenom Macrocycl Chem (2010) 66:307–314
DOI 10.1007/s10847-009-9626-6

ORIGINAL ARTICLE

Photophysical behaviour of 2-(dimethylamino)-fluorene in organised assemblies

Francisco García Sánchez · Manuel Algarra · J. Lovillo · Alfonso Aguilar · Aurora Navas Díaz

Received: 7 May 2009 / Accepted: 29 June 2009 / Published online: 10 July 2009

Abstract The effects of cyclodextrins and TX-100 micelles on the fluorescent properties of 2-(dimethylamino)-fluorene (DAF) were studied. The photophysical properties of DAF in the micelle aggregates and cyclodextrins were used to explain how the cavity might affect the dynamics of intramolecular charge transfer and the twisting of the molecule. Results obtained show that α-, β- and γ-cyclodextrins interact in a different way with DAF and different values of quantum yield, lifetimes and absorption and emission wavelength were obtained. Because a small interior cavity size, α-cyclodextrin do not show interaction with DAF. Quenching studies demonstrated that in Triton X-100 micelles, DAF molecules migrated to the non polar region.

Keywords Inclusion complex · 2-(Dimethylamino)-fluorene · Cyclodextrins · Triton X-100 · TICT effect

Introduction

Intramolecular charge transfer (ICT) emission in which a dialkylamino group acts as an electron donor has been a subject of several recent investigations [1–5]. Among them, the most interesting are twisted intramolecular charge transfer (TICT) processes. The concept put forward by Grabowski of a TICT state, or charge transfer reaction which is accompanied by a twisting motion and orbital decoupling of the phenyl acceptor ring from the dimethylamine donor group, is generally favoured [1, 6–8]. The formation of excited TICT state is recognized by a phenomenon of dual fluorescence exhibiting a large stokes shift emission in addition to the normal emission from the local excited (LE) state. Recently, planar intramolecular charge transfer (PICT) model has been proposed as an alternative to explain the presence of dual fluorescence of other related compounds. This model postulates a planar structure of the emissive CT state but does not involve state interaction [9].

The TICT effect depends of the polarity of the medium and the viscosity, thus the formation of inclusion complex with organized assemblies in aqueous solutions such as surfactants or cyclodextrins (CD), [10, 11], offering an non polar inside environment markedly different to that from bulk solutions, is expected to have a significant effect on the TICT process on the included compound.

The TICT behaviour of related compounds in CD such as *p*-dimethylaminobenzonitrile [12], *p*-dimethylaminobenzoic [13] and 2-aminodiphenyl ether [14] have been reported and demonstrated that was suppressed in the non polar medium.

At high polarity an ICT process to fluorescent species competes efficaciously with ISC that loses importance. At high polarity the TICT state and the triplet becomes closer in energy to the TICT singlet but, still are energy unfavorable compared with that of the lowest excited state TICT of the planar conformation, and the relaxation twisting and ISC will not take place. Thus, in polar aprotic solvents the emissive state is the TICT. Solvents of high dielectric constant and basic properties cause both ionization and dissociation of DAF. The two steps, ionization and dissociation, are influenced in different ways by solvents. In alcohols and water DAF exhibits an intermolecular

F. García Sánchez (✉) · M. Algarra · J. Lovillo · A. Aguilar · A. Navas Díaz
Department of Analytical Chemistry, Faculty of Science, University of Málaga, Campus de Teatinos s/n, 29071 Malaga, Spain
e-mail: f_garcia@uma.es

proton-transfer from the methylene group to the hydrogen-bonding solvent which produces the ionization of DAF. In the proton transfer excited state the negative charge localized on the methylene bridged is stabilized by the positive charge localized in the dimethylamine group. This full charge separation is most favorable in a twisted conformation, in which would rotate the donor orbital with respect to the acceptor orbital. Thus this state can be identified as a TICT state of low quantum yield. Organized assemblies such as micelles or cyclodextrins may influence the photophysical process of molecules in a highly interesting way. When the probes are transferred from the polar aqueous phase to relatively less polar organized environments, the reduction in polarity leads to a marked blue-shift of the TICT emission and a dramatic increase in the emission yields from both nonpolar and TICT emission. The sensitivity of the fluorescence quantum yield, fluorescence lifetime, and position of the probes emission is utilized to test the microenvironment of a number of organized assemblies. CDs with different cavity diameters have been used advantageously to sequester guest on the basis of size [15–17]. Through complete or partial inclusion of the guest within or as a result of association with the CDs, the guest molecule is often afforded some protection from external quenchers. Such external quenchers may take the form of dissolved oxygen or, in certain cases, H_2O_2 molecules.

Previous works demonstrate the influence of micellar solutions on the proton transfer equilibrium [18–20] and also noticed the suppression in the proton dissociation process which was ascribed to protection from –OH attack by the hydrophobic microenvironment of the CD cavity [21, 22].

In the present study the TICT process, in α-CD, β-CD and γ-CD and micellar solutions of Triton X-100 was carried out how the cavity might affect the dynamics of charge transfer and the twisting of 2-(dimethylamino)-fluorene (DAF) and whether it is caused by the reduced polarity within the cavity or to structural resistance to twisting. It is very probable that the dynamics in the interiors of the cavity are different from those of the rims. Quenching experiments that used either KBr or CH_2Br_2 were carried out to establish that the DAF had migrated into the micellar phase.

Materials and methods

Materials

The 10 mM stock solution of DAF (Fig. 1) analytical grade (Aldrich Chemical Co.) was prepared in 1,4-dioxan. Triton

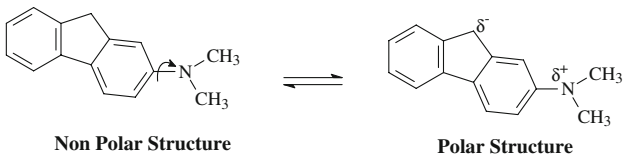

Fig. 1 Molecular structure of DAF

X 100 (TX-100), KBr, and CH_2Br_2 were purchased from Sigma. The α-, β- and γ-cyclodextrins (α-CD, β-CD and γ-CD, respectively) was a kind donation of Amaizo, USA. A 20 mM stock solution of TX-100 was prepared by dilution with double-distilled water. All other solvents were reagent grade (Merck). To introduce DAF into the micelles, 50 μL of 2×10^{-4} M DAF in dioxane were added to a series of TX-100 solutions whose micellar concentrations ranged from 0.05 to 1 mM. To introduce DAF into the cyclodextrins, 50 μL of 2×10^{-4} M DAF in dioxane were added to a series of α-CD, β-CD and γ-CD whose concentrations ranged from 5×10^{-4} to 0.1 M, 2.5×10^{-4} to 7.5×10^{-3} M, and 2.5×10^{-3} to 0.1 M, respectively. The samples were sonicated for 45 min at 25 °C.

Spectra fluorescence and lifetimes

Fluorescence and fluorescence-lifetimes were measured with an Aminco SLM 48000S spectrofluorimeter. The instrumentation is described in detail elsewhere [23]. The spectra were obtained by using a 1-nm scanning interval. The excitation monochromator entrance and entrance and exit slits of the emission monochromator were both 8 nm. Fluorescence-lifetimes were determined by using multifrequency-modulated excitation beams. A scattering-solution of glycogen was the reference. Measurements of the phase and modulation used the "100-average" mode in which each measurement was the average of 100 samplings. The excitation monochromator was set at 307 nm. We used the bandpass interference filter to eliminate all wavelengths below 340 nm. This filter was placed in the sample-emission receiving channel.

Heterogeneity analysis [24] was performed with SLM software, and used fluorescence-lifetime data recorded at six modulation frequencies. The rates of decay of intensity (I(t)) of the TX-100 samples were fitted to the multi-exponential model (Eq. 1):

$$I(t) = \sum \alpha_i e^{-\frac{t}{\tau_i}} \quad (1)$$

in which α_i represents the different amplitudes associated with the different decay times τ_i. The mean decay time τ is given by (Eq. 2) [24]:

$$\tau = \sum_{i} \alpha_i \tau_i \quad (2)$$

Fluorescence quantum yields

We measured the fluorescence quantum yields of DAF for a series of dioxane:water mixtures (0–100% of dioxane) and TX-100 and cyclodextrin samples. The procedure used to calculate φ is described by Marsh and Lowey [25], a known dilution of anthracene solution was made and a complete, uncorrected emission spectrum was recorded upon excitation at 307 nm. The absorbance at 307 nm of a solution of anthracene was then measured by using the 0.1 slide-wire of the spectrophotometer. This solution was transferred to a fluorescence cell, and a complete, uncorrected emission spectrum was recorded under the same optical conditions as for the DAF. The areas under the emission spectra were measured by using an electronic integrator and the quantum efficiency DAF was calculated from (Eq. 3):

$$\varphi_{DAF} = \frac{(\text{area under emission spectrum of DAF})}{(\text{area under emission spectrum of anthracene})} \times \frac{0.21\, A_{307}\ \text{anthracene}}{A_{307}\ \text{DAF}} \quad (3)$$

Calculation of nonradiative and radiative rates

Radiative rates (k_r) were derived from fluorescence quantum yield and lifetime of TICT emission (φ_{TICT} and τ_{TICT}, respectively, Eq. 4).

$$k_r = \frac{\varphi_{TICT}}{\tau_{TICT}} \quad (4)$$

We evaluated the rate constant k_{nr} for nonradiative decay from φ_{TICT} and the rate constant k_r [25]:

$$k_{nr} = k_r\left(\varphi_{TICT}^{-1} - 1\right) \quad (5)$$

Chang et al. [26] proposed a model to correct the solvent polarity effect on nonradiative decay in which k_{nr} is modified as follows, Eq. 6:

$$k_{cor} = k_{nr} \exp\left(-\frac{\beta[E_T(30) - 30]}{RT}\right) \quad (6)$$

in which k_{nr} is given by Eqs. 7 and 8.

$$k_{nr} = k_{nr}^{o} \exp\left(\frac{\beta[E_T(30) - 30]}{RT}\right) \exp\left(-\frac{E_B^o}{RT}\right) \quad (7)$$

$$\ln k_{nr} = B' + \frac{\beta}{RT}[E_T(30)] \quad (8)$$

If the corrected nonradiative rates (k_{cor}) tend to increase or decrease, several other factors not yet considered might be involved. A good correlation between k_{nr} and $E_T(30)$ will occur if k_{cor} values are randomly distributed within the experimental limits of uncertainty.

Results and discussion

Effects of cyclodextrins

The emission and excitation spectra of solutions of DAF in β-, and γ-CD are shown in Figs. 2 and 3, respectively. Tables 1 and 2 show the variation of emission properties of DAF as a function of cyclodextrin concentration. The λ_{em}, φ, and τ of the DAF in α-CD were independent of cyclodextrin concentration and the behavior of the DAF in α-CD was like that in aqueous solutions, which might be explained through shallow or noninclusional interactions of DAF with α-CD. While the effects of α-CD on the emission spectra are small, the emission characteristics of DAF change very dramatically on addition of β-CD and especially on addition of γ-CD. The wavelengths of excitation and emission and the shape of the emission spectra of DAF in γ-CD are similar with those in dioxane, the results suggest that DAF experiences a microenvironment of increasing nonpolarity as the γ-CD concentration is increased. This, in turn, provides strong evidence that DAF is transferred from the bulk aqueous environment into the nonpolar γ-CD cavity. The variation of the k_{nr} with the concentration de β-CD or γ-CD displays the trend towards decreasing values, Tables 1 and 2 show that in β-CD, k_{nr} fell from 3.76 to 1.45 s^{-1}, and in γ-CD from 3.76 to 1.21 s^{-1}. These values clearly indicate that the nonradiative processes are minimized when the CD concentration increases. The lifetimes of DAF progressively increase with the CD concentration, the long lifetime of DAF in γ-CD (5.71 ns) and β-CD (4.95 ns) compared with lifetimes in homogeneous media as hexane (2.91 ns), DMSO (4.84 ns), water (2.26 ns), protic solvents (4.37–2.26 ns), aprotic solvents (2.91–4.84 ns), and strongly viscous media (4.17 ns in glycerin at 0 °C) strongly support the

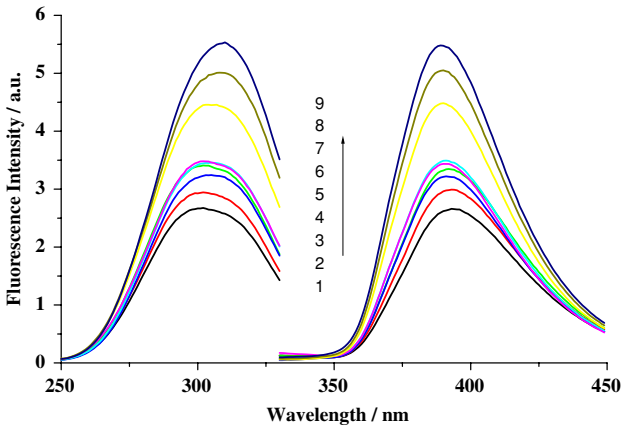

Fig. 2 Excitation and emission spectra of aqueous DAF solutions containing β-CD: (1) 0.0 M, (2) 10^{-4} M, (3) 2.5×10^{-4} M, (4) 5×10^{-4} M, (5) 7.5×10^{-4} M, (6) 10^{-3} M, (7) 2.5×10^{-3} M, (8) 5×10^{-3} M and (9) 7.5×10^{-3} M (λ_{ex} and λ_{em} are given in Table 1)

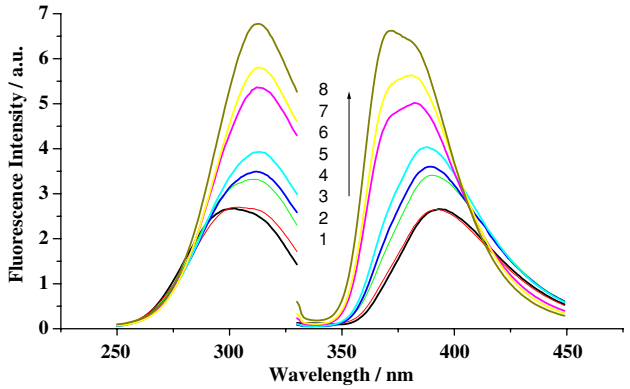

Fig. 3 Excitation and emission spectra of aqueous DAF solutions containing γ-CD: (1) 0.0 M, (2) 2.5×10^{-3} M, (3) 5×10^{-3} M, (4) 7.5×10^{-3} M, (5) 10^{-2} M, (6) 2.5×10^{-2} M, (7) 5×10^{-2} M and (8) 0.1 M (λ_{ex} and λ_{em} are given in Table 2)

hypothesis of the protection that offer the CDs, specially γ-CD, avoiding the deactivation of DAF. The long lifetimes implicate that the k_{nr} were smaller and that the proton dissociation is markedly decreased as a consequence of inclusion.

The decreasing in k_{nr} due to inclusion probably result from elimination of water molecules surrounding the fluorescent molecules suppressing the proton transfer process between DAF and the environment. This hypothesis is supported by assuming that in protic solvents emission occurs from both neutral (at 373 nm) and anionic (at 393 nm) forms of DAF in a proportion which depends of solvent basicity, thus in water, de more basic solvent, only the anionic form occurs. Data in Tables 1 and 2 suggest that the anion emission intensity decreases with CD concentration. This clearly indicates that the apparent excited state prototropic equilibrium is shifted towards the neutral form on inclusion in CD. Additionally, the inclusion probably decreases the intramolecular rotational freedom of these molecules by fixing them inside the cavity of CD, resulting in the decrease of k_{nr}. The least reduction of the k_{nr} with the β-CD concentration demonstrates the partial inclusion of DAF inside the β-CD cavity, permitting the rotation of the amino group and favoring the TICT process.

The short lifetime obtained in β-CD suggest that another mechanism of deactivation takes place. If the deactivation was only due to protonic transfer of the hydrogen methylenic of the moiety fluorene, this process would impeded same in β-CD and γ-CD, however the highest velocity observed in β-CD only can be due to deactivation through TICT process that is produced by partial inclusion an free rotation of $N(CH_3)_2$ group. In conclusion, DAF is not included in α-CD, while that β- and γ-CD is included with axial orientation. The smaller cavity of β-CD impedes the penetration of $N(CH_3)_2$ group remaining in contact with the aqueous phase and is free to rotate. From lifetimes and k_{nr} values are deduced that the interior of the cavity impedes the intermolecular proton transfer, being the neutral form of DAF which forms the complex.

Table 1 Photophysical properties of DAF at different concentrations of β-CD

[βCD] (M)	λ_{exc} (nm)	λ_{em} (nm)	τ (ns)	φ	10^{-7} Ak_r (s^{-1})	10^{-8} Ak_{nr} (s^{-1})
0.0	302	393	2.26	0.15	6.64	3.76
1.0×10^{-4}	302	393	2.52	0.16	6.35	3.33
2.5×10^{-4}	302	392	2.84	0.18	6.34	2.89
5.0×10^{-4}	305	391	3.22	0.17	5.28	2.58
7.5×10^{-4}	305	391	3.51	0.18	5.13	2.34
1.0×10^{-3}	302	390	3.76	0.18	4.79	2.18
2.5×10^{-3}	307	390	4.09	0.23	5.62	1.88
5.0×10^{-3}	308	390	4.82	0.26	5.39	1.54
7.5×10^{-3}	310	389	4.95	0.28	5.66	1.45

Table 2 Photophysical properties of DAF at different concentrations of γ-CD

[γCD] (M)	λ_{exc} (nm)	λ_{em} (nm)	τ (ns)	φ	10^{-7} Ak_r (s^{-1})	10^{-8} Ak_{nr} (s^{-1})
0.0	302	393	2.26	0.15	6.64	3.76
2.5×10^{-3}	306	392	3.51	0.15	4.27	2.42
5.0×10^{-3}	311	390	4.06	0.19	4.68	2.00
7.5×10^{-3}	312	389	4.25	0.20	4.71	1.88
10^{-2}	313	388	4.33	0.22	5.08	1.80
2.5×10^{-2}	312	380	5.25	0.26	4.95	1.41
5.0×10^{-2}	314	379	5.52	0.28	5.07	1.30
1.0×10^{-1}	312	370	5.71	0.31	5.43	1.21

Additionally the guest molecules in these cavities have often forced orientations and constrained conformations, DAF included totally in γ-CD decreases the deactivation through TICT process; however in β-CD, that no permits the total inclusion of DAF, the TICT deactivation is favored.

Micellar effects

TX-100 belongs to a non-ionic surfactant group so it may be expected no influence on protonation occur due to the charge on the micelle. The critical micellar concentration (CMC) is the concentration above which micelles form and above which both monomers and micelles exist in dynamic equilibrium [27–29]. In aqueous, non-ionic detergent solutions below CMC, small aggregates (usually dimmers or trimmers) form because there is no electrostatic repulsion between their head-groups and because of this steric repulsion predominates.

Fluorescence spectroscopy and lifetime

We recorded the excitation and fluorescence excitation and emission spectra of DAF for a series of 11 mixtures that contained a fixed concentration of DAF (10^{-6} M) and different concentrations of TX-100. Figure 4 shows the excitation and emission spectra. When the concentration of TX-100 was increased the fluorescence of the ICT state progressively intensified and shifted towards the blue. The DAF λ_{exc} and λ_{em} for eleven different TX-100 concentrations are given in Table 3. The results of the fluorescence-lifetime determinations and of the heterogeneity analyses are summarized in Table 3. Lifetimes were determined for

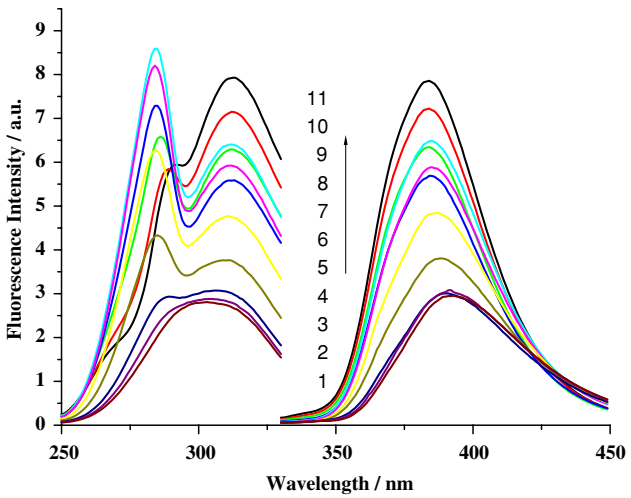

Fig. 4 Excitation and emission spectra of aqueous DAF solutions containing TX-100 : (1) 0.05 mM, (2) 0.1 mM, (3) 0.15 mM, (4) 0.2 mM, (5) 0.25 mM, (6) 0.30 mM, (7) 0.35 mM, (8) 0.40 mM, (9) 0.60 mM, (10) 0.80 mM, and (11) 1.0 mM

fixed concentrations of DAF (10^{-6} M) and different TX-100 concentrations (0.1–1.0 mM). The lifetimes of the fixed DAF concentrations showed heterogeneity for most of the different concentrations of TX-100. The two concentrations below 0.1 mM of TX-100 had single, short and constant lifetimes. At TX-100 concentrations of 0.15 mM and above, a second, long-lived signal appeared and its fractional contribution to the intensity increased as a function of the TX-100 concentration. TX-100 concentrations above 0.8 mM DAF showed large constant lifetimes.

These progressive changes of the fractional lifetime contributions suggest that small aggregates had formed below the CMC and that the DAF was mostly in a nonpolar microenvironment. Figure 5 depicts the dependence between the concentration of TX-100 and $\ln(1/\tau)$. Above 0.6 mM, $\ln(1/\tau)$ was practically independent of concentration. By linear fitting the two regions and calculating the point of intersection we obtained a CMC value of 0.33 mM for TX-100. This value agrees well with those in the literature [28–30]. Because reductions in solvent polarity caused a blue-shift of the emission, we tested the correlations of λ_{em} for a series of eleven dioxane:water mixtures. The correlation between λ_{em} and $E_T(30)$ was 0.9938 (r); the regression line slope was 0.85, and the intercept was at 339.74 nm. We calculated the $E_T(30)$ value for each mixture by comparing the λ_{em} obtained for DAF at several concentrations of TX-100 (Table 3). We knew that at TX-100 concentrations below 0.25 mM, the DAF was located in a polar microenvironment with an $E_T(30) = 56.3$ Kcal mol^{-1}. Above CMC, $E_T(30)$ was practically constant, the mean of our data was 58.2 Kcal mol^{-1}.

We determined $E_T(30)$ by employing the TICT process and it corresponded closely to the polarity values within the interior of the micelle given by Kalyanasundaram [31] who uses solutions of pyrene in different solvents and then calculates the corresponding ratios between bands I and III of the fluorescence spectra.

All these results suggest that DAF is dissolved in the interior of the micelle. The k_r and k_{nr} in Table 3 were calculated from τ and (. Least-squares analysis of k_{nr} gave β/RT = 0.086 mol Kcal^{-1} and $\beta = 0.051$. These values were smaller than the β/RT and β given by dioxane:water mixtures. However, these results suggest that the TICT state in micellar media is less favored than in dioxane:water mixtures. The k_{cor} values (Table 3), were obtained in a similar way. The variations of the calculated k_{cor} in TX-100 micelles were reasonably random their mean values were around 2.36 $\times 10^7$ s^{-1}, the standard deviation was 0.17 $\times 10^7$ s^{-1}. Between 0.05 and 0.30 mM of TX-100, the means of the k_{cor} values of samples containing more than 0.30 mM of TX-100 was 1.85 $\times 10^7$ s^{-1} and the standard deviation was about 0.16 $\times 10^7$ s^{-1}. The low k_{cor} above the CMC suggest that the TICT process was retarded,

Table 3 Photophysical properties of DAF at different concentrations of TX-100

[TX-100] (mM)	λ_{exc} (nm)	λ_{em} (nm)	τ^a (ns)	φ	10^{-7} Ak_r (s^{-1})	10^{-8} Ak_{nr} (s^{-1})	10^{-6} Ak_{nr} (s^{-1})	$\tau_1(\alpha_1)^b$ (ns)	$\tau_2(\alpha_2)^b$ (ns)
0.05	303	393	2.25	0.16	7.11	2.22	3.78	2.25 (1.000)	–
0.10	305	392	2.35	0.17	7.23	2.32	3.73	2.35 (1.000)	–
0.15	306	390	2.55	0.19	7.45	2.56	3.53	2.05 (0.739)	4.15 (0.261)
0.20	311	388	3.04	0.21	6.91	2.57	3.18	2.05 (0.620)	5.06 (0.380)
0.25	312	387	3.83	0.23	6.00	2.20	2.60	2.21 (0.472)	5.28 (0.528)
0.30	312	385	4.42	0.25	5.66	2.27	2.01	1.85 (0.257)	5.30 (0.743)
0.35	312	385	4.82	0.26	5.39	2.06	1.70	2.39 (0.294)	5.95 (0.706)
0.40	312	385	5.11	0.28	5.48	1.89	1.54	2.02 (0.182)	5.71 (0.818)
0.60	312	384	5.41	0.31	5.73	1.90	1.41	2.34 (0.144)	5.83 (0.856)
0.80	312	384	5.53	0.35	6.33	1.75	1.28	–	5.53 (1.000)
1.00	312	384	5.64	0.38	6.74	1.63	1.18	–	5.64 (1.000)

[a] Lifetime calculated by unimodal Gaussian distributions

[b] Within parenthesis fractional intensity contributions, calculated by two components heterogeneity analysis

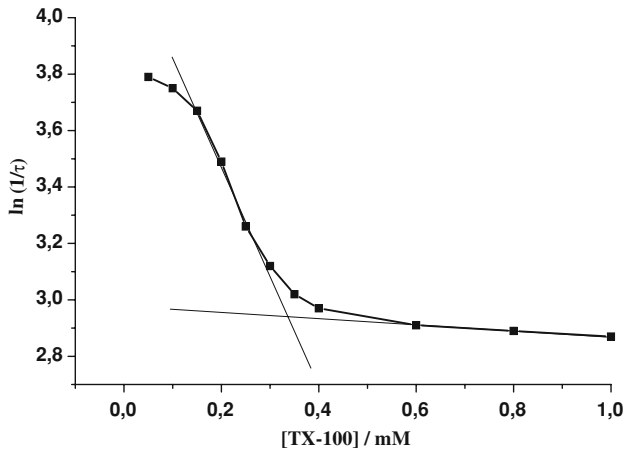

Fig. 5 Effect of TX-100 concentration on the lifetime of DAF

probably because of the restrictions imposed by the interior of the micelle. The hydrophobic interior markedly decreased the intermolecular proton transfer and the restricted geometry impedes TICT originating the highest lifetimes measured (5.95 ns).

Quenching studies

To localize definitely the DAF in the micelle, we carried out quenching studies with two different quenchers, one neutral dibromomethane (CH_2Br_2), and the other ionic (KBr). The range of concentrations was such that the following conventional Stern–Volmer equation was obeyed [24].

$$I_o/I = 1 + K_{sv}[Q]$$

in which I_o and I are the respective fluorescence intensities in the absence of and presence of the quencher, K_{sv} is the Stern–Volmer constant, and [Q] is the quencher concentration.

We measured the fluorescence intensities of different mixtures of TX-100, DAF and quencher for fixed concentration of DAF and TX-100 while progressively increasing quencher concentration. We repeated this procedure for several different TX-100 concentrations. Figure 6a, b shows the plots of I_o/I as function of quencher concentration for KBr and CH_2Br_2, respectively. When we used the KBr ionic quencher, it is found that the fluorescence intensity of DAF was quenched at sub-CMC concentrations of TX-100. On the other hand, the CH_2Br_2 quenched the fluorescence above CMC. K_{sv} constant values (an index of quenching efficiency) obtained from the slope of the plots I/I_0 against quencher concentration was found to be 9×10^{-4} M^{-1} for 0.0 and 0.1 mM TX-100, and 3×10^{-6} M^{-1} for 0.4 mM TX-100, in the case of KBr ionic quencher. As can be seen in Fig. 6a the DAF molecule was quenched at sub-CMC concentrations (CMC = 0.33 mM) and not quenched above CMC. This fact indicates that DAF migrates to micellar core and impedes the encounters quencher/DAF because hydrophilic nature of quencher. In the case of neutral quencher (Fig. 6b) it was found K_{sv} values of 19.8×10^{-3} M^{-1} (0.1 M TX-100) and 1.13 M^{-1} (0.4 mM TX-100). Above CMC quenching efficiency is dramatically enhanced supporting the hypothesis that both quencher and DAF are included into micelle core affecting the dynamic distribution of these species during the time scale of fluorescence quenching. These results demonstrate clearly that DAF had migrated into the nonpolar region of TX-100.

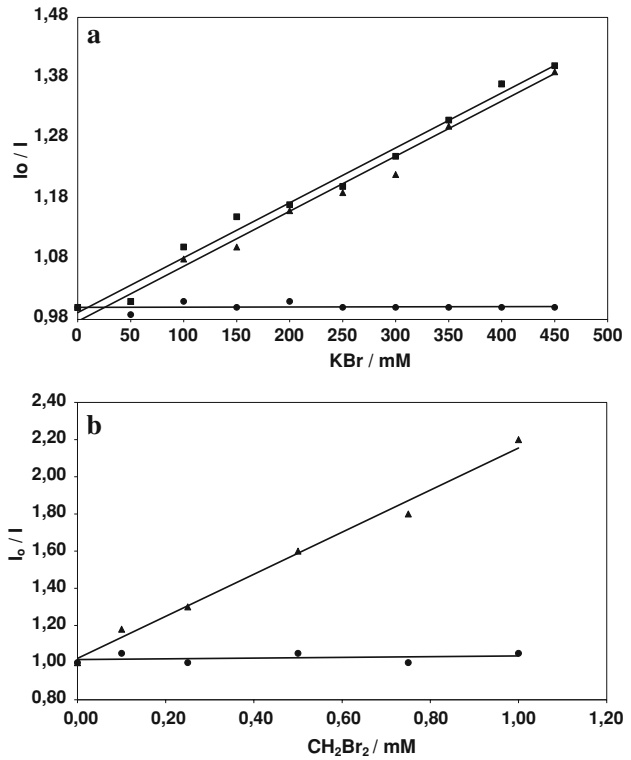

Fig. 6 Quenching studies. **a** Effect of KBr concentration on the fluorescence intensities of DAF at three TX-100 concentrations (*filled circle*) 0.4 mM, (*filled triangle*) 0.1 mM and (*filled square*) 0 mM. **b** Effect of CH_2Br_2 concentration on fluorescence intensities of DAF at two TX-100 concentrations: (*filled circle*) 0.1 mM, (*filled triangle*) 0.4 mM

Conclusions

Time resolved and steady state fluorescence studies show that cyclodextrin apolar cavities can accommodate DAF molecules in a different manner according with internal cavity size. Emission and excitation wavelength, lifetime, quantum yield and non radiative constants give adequate information about the DAF behaviour in presence of cyclodextrins. Quenching studies that use ionic or non-ionic quenchers demonstrate that the TX-100 micelles provide in their interior a host microenvironment for the DAF molecules. The fluorescence spectra and the non-radiative rates reveal that DAF were confined within the micellar interiors.

References

1. Rettig, C.: Charge separation in excited-states of decoupled systems—TICT compounds and implications regarding the development of new laser-dyes and the primary processes of vision and photosynthesis. Angew. Chem. Int. Ed. Engl. **25**, 971–986 (1986)
2. Grabowski, Z.R., Rotkiewicz, K., Rettig, C.: Structural changes accompanying intramolecular electron transfer: focus on twisted intramolecular charge-transfer states and structures. Chem. Rev. **103**, 3899–4031 (2003)
3. Hazra, P., Chakrabarty, D., Sarkar, N.: Intramolecular charge transfer and solvation dynamics of coumarin 152 in aerosol-OT, water-solubilizing reverse micelles, and polar organic solvent solubilizing reverse micelles. Langmuir **18**, 7872–7879 (2002)
4. Jiang, Y.B.: Effect of cyclodextrin inclusion complex formation on the twisted intramolecular charge-transfer (TICT) of the included compound the p-dimethylaminobenzoic acid-β-cyclodextrin. J. Photochem. Photobiol. A **88**, 109–116 (1995)
5. Panja, S., Chakravorti, S.: Photophysics of 4-N,N dimethylamino cinnamaldehyde in AOT reverse micelles and exploration of its position and orientation. Chem. Phys. Lett. **367**, 330–338 (2003)
6. Herbich, J., Karpiuk, J., Grabowski, Z.R., Tamai, N., Yoshihara, K.: Modification of the intramolecular electron-transfer by hydrogen-bonding 4-(dialkylamino)pyrimidines. J. Lumin. **54**, 165–175 (1992)
7. Druzhinin, S.I., Demeter, A., Zachariasse, K.A.: Dual fluorescence and intramolecular charge transfer with crystalline 4-(diisopropylamino)benzonitrile. Chem. Phys. Lett. **347**, 421–428 (2001)
8. Hazra, P., Chakrabarty, D., Chakraborty, A., Sarka, N.: Effect of hydrogen bonding on intramolecular charge transfer in aqueous and non-aqueous reverse micelles. J. Photochem. Photobiol. A **167**, 23–30 (2004)
9. Zachariasse, K.A.: Comment on Pseudo-Jahn-Teller and TICT-models: a photophysical comparison of meta-and para-DMABN derivatives. The PICT model for dual fluorescence of aminobenzonitriles. Chem. Phys. Lett. **320**, 8–13 (2000)
10. Szjetli, J.: Cyclodextrins and their Inclusion Complexes. Akademiai Kiado, Budapest, Hungary (1982)
11. Dodziuk, H.: Cyclodextrin and their Complexes Chemistry, Analytical Methods, Applications. Wiley-VCH, Weinheim, Netherlands (2000)
12. Nag, A., Bhattacharyya, K.: Twisted intramolecular charge transfer emission of dimethylaminobenzonitrile in α-cyclodextrine cavities. Chem. Phys. Lett. **151**, 474–476 (1988)
13. Jiang, Y.B., Lin, L.: Dual fluorescence of *p*-dimethylaminobenzoic acid in ctyltrimethylammonium bromide (CTAB)/1-heptanol/water reverse micelle. Appl. Spectrosc. **49**, 1017–1021 (1995)
14. Muthu, I.V., Enoch, V., Swaminathan, M.: Flourimetric and prototropic studies on the inclusion complexation of 2-amino and 4-aminodiphenyl ethers with β-cyclodextrin: unusual behavior of 4-aminodiphenyl ether. J. Lumin. **127**, 713–720 (2007)
15. García Sánchez, F., Navas Díaz, A., Fernández Correa, R.: Spectrofluorimetric determination of the herbicide bentazone: microenvironmental effects on the analytical signal. Anal. Chim. Acta **259**, 61–66 (1992)
16. García Sánchez, F., Navas Díaz, A., Lovillo, J., Feria, L.S.: α-Cyclodextrin as a restricted access mobile phase for reversed-phase liquid chromatography with fluorimetric detection of phenolic compounds. Anal. Chim. Acta **328**, 73–79 (1996)
17. Heredia, A., Requena, G., García Sánchez, F.: An approach for the estimation of the polarity of the β-cyclodextrin internal cavity. J. Chem Soc. Chem. Commun. **24**, 1814–1815 (1985)
18. Moulik, S.P., Ray, S., Das, A.R.: Interaction of p-nitrosalicylic acid with ethylenediamine in presence of cetyltrimethylammonium bromide, sodium dodecylsulfate, Triton X-100, polyethylene-glycol and their binary-mixtures-proton donor-acceptor equilibrium in micellar solution. J. Phys. Chem. **81**, 1766–1773 (1977)
19. Abou-Al Einin, S., Zaitsev, A.K., Zaitsev, N.K., Kuzmin, M.G.: Photoprotolytic dissociation in micellar solutions. J. Photochem. Photobiol. A **41**, 365–373 (1988)

20. Lin, L.R., Jiang, Y.B., Huang, X.Z., Chen, G.Z.: Cyclodextrin effect on micellization of cetryl ammonium bromide in aqueous solution. Probed by dual fluorescence of dimethylaminobenzoate. Spectr. Lett. **30**, 1551–1560 (1997)
21. Yorozu, T., Hoshino, M., Imamura, M., Shizuka, H.: Photoexcited inclusion complexes of β-naphthol with α-cyclodextrin, β-cyclodextrin, and γ-cyclodextrin in aqueous-solutions. J. Phys. Chem. **86**, 4422–4426 (1992)
22. Eaton, D.F.: Cyclodextrin complexation as a probe of molecular photophysics. Tetrahedron **43**, 1551–1570 (1987)
23. García Sánchez, F., Navas, A., Lovillo, J., Baro, E., Algarra, M.: Resolution of (+)-cinchonine and (−)-cinchonidine by phase-modulation fluorescence spectroscopy. Anal. Chim. Acta **639**, 67–72 (2009)
24. Lakowicz, J.R.: Principles of Fluorescence Spectroscopy, 3rd edn. Springer, New York (2006)
25. Marsh, D.J., Lowey, S.: Fluorescence energy transfer in myosin subfragment-1. Biochemistry **19**, 774–784 (1980)
26. Chang, T.L., Cheung, H.C.: A model for molecules with twisted intramolecular charge-transfer characteristics-solvent polarity effect on the nonradiative rates of dyes in a series of water ethanol mixed-solvents. Chem. Phys. Lett. **143**, 343–348 (1990)
27. McBain, J.W.: Solubilization and other factors in detergent action. Adv. Colloid Sci. **1**, 99–142 (1942)
28. García Sánchez, F., Carnero Ruíz, C.: Energy transfer in Triton X-100 micelles. J. Lumin. **55**, 321–325 (1993)
29. Carnero Ruíz, C., García Sánchez, F.: Effect of urea on aggregation behavior of Triton X-100 micellar solutions-a photophysical study. J. Colloid Interface Sci. **165**, 110–115 (1994)
30. Kano, K., Ueno, Y., Umakoshi, S., Ishibashi, T., Ogawa, T.: Freeze-thaw effect on solubilization of hydrophobic compounds in micelles and artificial bilayer membranes. J. Phys. Chem. **88**, 5087–5092 (1984)
31. Kalyanasundaram, K., Thomas, J.K.: Environmental effects on vibronic band intensities in pyrene monomer fluorescence and their application in studies of micellar systems. J. Am. Chem. Soc. **99**, 2039–2044 (1977)